Characterization of Complexes between *Escherichia coli* Sulfite Reductase Hemoprotein Subunit and Its Substrates Sulfite and Nitrite†

Peter A. Janick,‡ David C. Rueger,§ Rick J. Krueger,⊥ Michael J. Barber, and Lewis M. Siegel*

ABSTRACT: The hemoprotein subunit (SiR-HP) of *Escherichia coli* NADPH–sulfite reductase when fully reduced reacts rapidly with NO_2^- or SO_3^{2-} to give spectroscopically distinct stable complexes. The reaction, which proceeds rapidly enough to be of significance in catalysis, is a two-step process. The first step (ca. 17 s^{-1}) involves replacement of the EPR signals characteristic of reduced Fe_4S_4 centers exchange coupled to $S = 1$ or 2 ferroheme with a signal of the "$g = 1.94$" type characteristic of magnetically isolated reduced Fe_4S_4. The second step (ca. 100 s^{-1}) is much faster and presumably involves electron transfer from the reduced Fe_4S_4 center to the heme–substrate complex. With NO_2^-, the final species formed exhibits an EPR spectrum characteristic of ferroheme–NO complexes; its optical maxima are at 400 and 599 nm. Two distinct EPR species are present: the majority species is rhombic ($g = 2.117$, 2.008, and 1.996) with distinct hyperfine splitting due to NO, while the minority species is relatively axial, with its high field $g = 2.068$. (Formation of SiR-HP ferroheme–NO complex in the presence of 2 M urea or 60% (v/v) dimethyl sulfoxide causes the axial spectrum to predominate. The EPR spectrum of plant nitrite reductase ferroheme–NO closely resembles the axial "$g = 2.07$" species of SiR-HP–NO. With SO_3^{2-}, the final species formed exhibits optical maxima at 396 and 592 nm but is EPR silent.) The complexes formed between fully reduced SiR-HP and substrates can be oxidized by $Fe(CN)_6^{2-}$ to yield EPR silent species with the following optical maxima: oxidized SiR-HP–NO_2^-, 399 and 581 nm; oxidized SiR-HP–SO_3^{2-}, 408 and 583 nm. The oxidized SiR-HP–NO_2^- can be reduced to the ferroheme–NO species with ascorbate. The oxidized SiR-HP–SO_3^{2-} complex ($K_d = 7$ μM) has also been formed on reaction of SO_3^{2-} with fully oxidized SiR-HP or enzyme in the presence of limiting amounts of reduced methylviologen (MV^+). The bound S, released in 3.3 M urea, is at the oxidation level of SO_3^{2-}. Binding of SO_3^{2-} (or CN^-) to oxidized SiR-HP is a two-step process. At least one step is independent of the concentration of added ligand: $k = 5.8 \times 10^{-5}$ s^{-1} for SO_3^{2-} and 14×10^{-5} s^{-1} for CN^-. SO_3^{2-} dissociation from oxidized SiR-HP–SO_3^{2-} is also slow, $k_{off} = 6 \times 10^{-6}$ s^{-1}. The rate of ligand binding to or dissociation from SiR-HP is markedly increased by addition of about 1 mol of MV^+/mol of SiR-HP. At such low MV^+/heme ratios, the SiR-HP–SO_3^{2-} complex is dissociated to yield free SO_3^{2-} and little or no H_2S. As the MV^+/heme ratio is increased, the bound SO_3^{2-} becomes stoichiometrically reduced to H_2S. When reaction of SiR-HP-$^{35}SO_3^{2-}$ complex by excess MV^+ was carried out in the presence of a 250-fold excess of nonradioactive SO_3^{2-}, 24% of the bound ^{35}S was reduced to $H_2{}^{35}S$. Thus the rate of reduction of bound SO_3^{2-} is of the same order of magnitude as the rate of its dissociation from the reduced enzyme.

The siroheme–Fe_4S_4 center enzymes, sulfite reductase (SiR)[1] and nitrite reductase (NiR), each catalyze the six-electron reductions of SO_3^{2-} to H_2S and NO_2^- to NH_3 (Lancaster et al., 1979; Krueger & Siegel, 1982; Siegel et al., 1982). The most extensively studied of these enzymes, the monomeric hemoprotein subunit (SiR-HP) derived by urea dissociation of the oligomeric *Escherichia coli* NADPH–sulfite reductase hemoflavoprotein complex (Siegel & Davis, 1974), contains an active center in which the heme and Fe_4S_4 groups are magnetically exchange coupled, i.e., chemically linked by a common bridging ligand, in the native enzyme (no added ligands; Christner et al., 1981; Janick & Siegel, 1982). There is also strong evidence for prosthetic group interaction, consistent with maintenance of the coupling, in SiR-HP containing tightly bound heme ligands, such as CN^- (Janick & Siegel, 1983). Christner et al. (1981) have reported preliminary Mössbauer evidence which indicates that the siroheme and Fe_4S_4 centers of spinach NiR are exchange coupled as well. It is obviously of interest to examine the interaction of this active center with substrates.

Siegel et al. (1982) have reported that SiR-HP (which catalyzes the six-electron reductions of both SO_3^{2-} and NO_2^-, at rates comparable to the NADPH–SiR hemoflavoprotein, when supplied with the artificial reductant MV^+) can form a tight 1:1 complex with SO_3^{2-}. This complex, which was formed in the presence of small amounts of MV^+, has not been well characterized. Similarly, Lancaster et al. (1979) showed that spinach NiR forms a 1:1 complex with NO_2^-. In the presence of a reductant, this interaction leads to the production of a ferroheme–NO species with a relatively axial type of EPR spectrum (Cammack et al., 1978; Lancaster et al., 1979; Fry et al., 1980).

In the present work, we report on a number of EPR and optical spectroscopic properties of stable complexes formed between fully reduced SiR-HP and its substrates SO_3^{2-} and NO_2^- and of more oxidized forms of these complexes. We have characterized the oxidized SiR-HP–SO_3^{2-} complex in some

† From the Department of Biochemistry, Duke University School of Medicine, and the Veterans Administration Hospital, Durham, North Carolina 27705. *Received July 6, 1982.* This work was supported by Grant AM-13460 from the National Institutes of Health, Grant PCM-7924877 from the National Science Foundation, and Project Grant 7875-01 from the Veterans Administration.

* Address correspondence to this author at the Department of Biochemistry, Duke University Medical Center.

‡ Part of this work is from dissertations submitted by P.A.J. and D.C.R. to Duke University in partial fulfillment of the requirements for the degree of Doctor of Philosophy. P.A.J. is a fellow of the Medical Scientist Training Program at Duke University.

§ Present address: Spinal Cord Injury Research Department, West Roxbury Veterans Administration Medical Center, West Roxbury, MA 02132.

⊥ Present address: Department of Chemistry, Massachusetts Institute of Technology, Cambridge, MA 02139.

[1] Abbreviations: Dfl, 5′-deazaflavin; EDTA, ethylenediaminetetraacetic acid; Fe_4S_4, tetranuclear iron–sulfur center; Me_2SO, dimethyl sulfoxide; MV^{2+}, oxidized methylviologen; MV^+ (or MVH), methylviologen cation radical; NiR, nitrite reductase; SiR, sulfite reductase; SiR-HP, hemoprotein subunit of *E. coli* NADPH–sulfite reductase hemoflavoprotein complex; GdmCl, guanidinium chloride.

0006-2960/83/0422-0396$01.50/0

detail. We have also conducted kinetic studies which show that reaction of either two-electron-reduced or -oxidized SiR-HP with substrate involves a minimum of two steps. With the reduced (but not oxidized) enzyme, both of these steps occur rapidly enough to permit their participation in the six-electron reductions catalyzed by the enzyme.

Experimental Procedures

Buffer. The "standard buffer" used throughout the present work was 0.1 M potassium phosphate–0.1 mM EDTA, pH 7.7.

Enzyme. E. coli NADPH–SiR was purified by the procedure of Siegel et al. (1973). The SiR-HP subunit was dissociated and isolated as described by Siegel & Davis (1974), except that 4 M urea was used in the current procedure to minimize loss of prosthetic groups. SiR-HP concentration was determined spectrophotometrically by using an extinction coefficient at 591 nm of 1.8×10^4 M^{-1} cm^{-1} (Siegel et al., 1982).

Reduced Methylviologen and Enzyme Assays. Solutions of methylviologen chloride (K & K Laboratories) in standard buffer were reduced with H_2/Pt asbestos (such solutions are approximately 50% MV^+ and 50% MV^{2+}). For details and for the method used to assay MV^+–SO_3^{2-} reductase activity, see Krueger & Siegel (1982). The extinction coefficient used for MV^+ was 1.3×10^4 M^{-1} cm^{-1} at 600 nm (Thorneley, 1974). Anaerobic conditions used throughout this work were as described by Krueger & Siegel (1982) and Siegel et al. (1982).

Chemical Measurements. Measurements of SO_3^{2-} and S^{2-} concentrations, of the specific radioactivity of $Na_2{}^{35}SO_3$ (New England Nuclear) solutions and of $H_2{}^{35}S$ concentrations, were as described by Krueger & Siegel (1982). Determinations of cyanide concentrations and of the specific radioactivity of $K^{14}CN$ (Amersham/Searle) solutions were as described by Siegel et al. (1982).

For removal of low molecular weight solutes in ligand binding experiments, 0.5–2.0-mL samples were applied to a column (1.5 × 2.5 cm) of Sephadex G-25 (fine) and 1.4-mL fractions collected at flow rates of approximately 50 mL/h. Fractions were analyzed for radioactivity, in scintillation mixtures on a Packard 3375 TriCarb liquid scintillation spectrometer, and for protein by the microbiuret procedure of Zamenhof (1957).

Spectra. Absorption spectra were recorded at 22 °C in silica cells of 1-cm path length with either an Aminco DW-2 or a Cary Model 14 spectrophotometer. EPR spectra were recorded on frozen samples with a Varian E9 spectrometer operating at X band with field modulation of 100 kHz. Temperature was maintained by means of an Air Products liquid He cryostat. Spin concentrations were determined under nonsaturating conditions by double integration with CuEDTA as standard (Aasa & Vangaard, 1975). The ferroheme–NO signal was measured at 35 K and 5 mW. For other signals see Janick & Siegel (1983).

Spectrophotometric Determination of SiR-HP–SO_3^{2-} and SiR-HP–CN^- Complexes. The fraction of SiR-HP present as the sulfite complex was determined spectrophotometrically in some experiments from the ratio of the absorbance at 386 nm (absorption maximum wavelength for free SiR-HP) to that at 402 nm (a wavelength isosbestic for the free and complexed SiR-HP) by means of the equation

$$[\text{SiR-HP–SO}_3^{2-}]/[\text{SiR-HP}]_{\text{total}} = [1.162 - (A_{386}/A_{402})]/0.278$$

This equation is based on the fact that the A_{386}/A_{402} ratios of the free SiR-HP and its SO_3^{2-} complex are 1.162 and 0.884, respectively, and assumes that the only absorbing species present are these two enzyme forms. Similarly, the fraction of SiR-HP present as the cyanide complex in a given sample was determined from the equation

$$[\text{SiR-HP–CN}^-]/[\text{SiR-HP}]_{\text{total}} = [1.195 - (A_{386}/A_{404})]/0.369$$

which derives from the fact that the spectra of the free oxidized SiR-HP and its cyanide complex are isosbestic at 404 nm and have A_{386}/A_{404} ratios of 1.195 and 0.835, respectively. See Siegel et al. (1982) for the relevant spectra.

Photoreduction of SiR-HP. Anaerobic photoreduction of SiR-HP solutions in EPR tubes or optical cuvettes was achieved by the method of Massey & Hemmerich (1978). Enzyme solutions contained 10 mM EDTA and Dfl/SiR-HP ratios of 0.2–0.4. Dfl was a generous gift of Dr. D. Seybert. For details of the photoreduction procedure, the anaerobic techniques employed, the methods for recording optical and EPR spectra of enzyme samples during the photoreduction process, and the procedures for determining the number of electrons in a particular photoreduced enzyme sample by titration with ferricyanide, see Janick & Siegel (1982).

Rapid Kinetics. Freeze-quenched samples were prepared for EPR analysis by mixing equal volumes of anaerobic solutions of substrate and fully photoreduced SiR-HP with an Update Instruments System 1000 precision ram system. After an appropriate reaction time, determined by the length of tubing through which the mixed solution is required to pass, samples were dispersed by passage through a narrow orifice and collected in tubes containing isopentane at −140 °C. For details of the procedure see Bray (1961) and Barber & Salerno (1980).

Results

Nitrosyl Complexes of SiR-HP. Although heme–NO complexes have often been formed by saturating heme (either ferric or ferrous) solutions with NO gas, we have found SiR-HP in the oxidized state to be relatively unreactive toward the usual heme ligands (see below). Oxidized SiR-HP does react with NO to form a complex (with the 581-nm absorption maximum described below), but this reaction requires about 3 days to reach 50% completion. No reaction between oxidized SiR-HP and NO_2^- has been detected. Since the midpoint potentials for reduction of the Fe_4S_4 center and heme of unligated SiR-HP are relatively close together [−405 and −340 mV, respectively; see Janick & Siegel (1982)], it is not possible to obtain enzyme completely in the state ferroheme–oxidized Fe_4S_4 even when the enzyme contains an average of one electron per SiR-HP. Thus, complexes between ferroheme SiR-HP and NO_2^- (equivalent in oxidation state to ferriheme–NO) are not readily prepared in relatively pure form by simple reaction of NO_2^{2-} with SiR-HP reduced to the one-electron state. However, since NO is one electron more reduced than NO_2^-, addition of NO_2^- to fully reduced (two-electron) SiR-HP is formally equivalent to addition of NO to one-electron enzyme (assuming that electron transfer from the reduced Fe_4S_4 center to the enzyme-bound NO_2^- is possible; that this can indeed occur will be shown below).

Figure 1 shows that NO_2^- does readily react with fully reduced SiR-HP to form a species with optical absorption maxima at 400 and 599 nm. [This spectrum, with its intense "hemochromogen" type peak at about 600 nm, is nearly identical with that seen on reaction of ferrous siroheme, whether free or enzyme bound, with CO (Siegel et al., 1978; Stolzenberg et al., 1981).] The EPR spectrum of this species

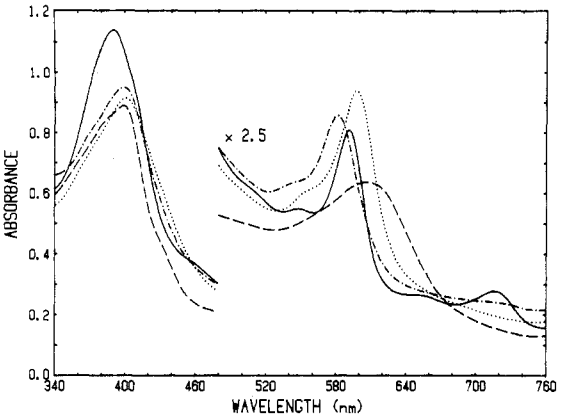

FIGURE 1: Optical spectra of complexes between SiR-HP and nitrite. Solutions containing 62 μM SiR-HP, 15 μM Dfl, and 10 mM EDTA in standard buffer in a total volume of 0.2 mL were made anaerobic in EPR tubes. Optical spectra were recorded in the EPR tubes, and additions were made anaerobically by means of a gas-tight syringe. Spectra have been corrected for dilution. (—) Oxidized SiR-HP. (---) Fully reduced SiR-HP (the solution was illuminated for 10 min; no optical change was observed during the last 3 min of illumination). (···) Fully reduced SiR-HP after addition of 10 μL of 0.1 M KNO_2. (-·-) Fully reduced SiR-HP to which 10 μL of 0.1 M KNO_2 and then 2.0 equiv of $K_3Fe(CN)_6$ were added.

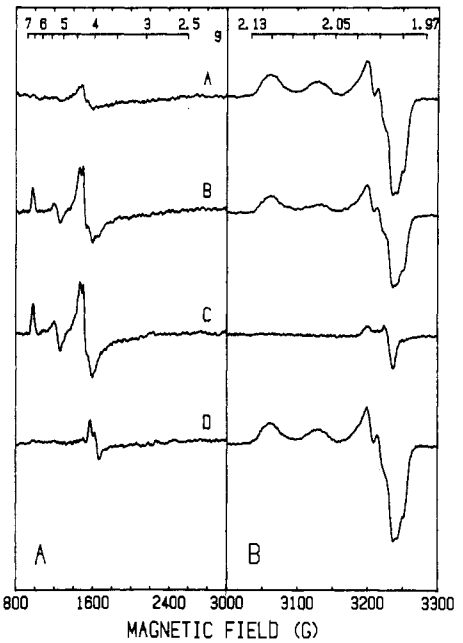

FIGURE 2: EPR spectra of complexes between SiR-HP and nitrite. Samples were prepared as described in Figure 1 and frozen in liquid N_2 for EPR analysis. (A) Fully reduced SiR-HP plus 10 μL of 0.1 M KNO_2; (B) fully reduced SiR-HP to which 10 μL of 0.1 M KNO_2 and then 1.0 equiv of $K_3Fe(CN)_6$ per SiR-HP were added; (C) fully reduced SiR-HP to which 10 μL of 0.1 M KNO_2 and then 2.0 equiv of $K_3Fe(CN)_6$ per SiR-HP were added; (D) fully reduced SiR-HP to which 10 μL of 0.1 M KNO_2 was added and the solution then illuminated for an additional 15 min (no change was detected in the optical spectrum). The low-field portion of the spectrum was recorded at a temperature of 18 K, 10 mW microwave power, and 10 G modulation amplitude. The high-field portion of the spectrum was recorded at a temperature of 35 K, 5 mW microwave power, and 4 G modulation amplitude. Microwave frequency was 9.12 GHz.

(Figure 2A) yields signals at g = 2.12, 2.07, 2.01, and 1.996; these signals taken together integrate to about 0.8 spin/SiR-HP (Table I). As seen in Figure 3, the triplet splitting of the g = 2.01 resonance is consistent with hyperfine coupling of the EPR signal to a single ^{14}N nucleus. Isotopic substitution with $^{15}NO_2^-$ leads to a doublet splitting of the g = 2.01 resonance, which confirms the presence of a single NO_2^--derived

Table I: Amounts of g = 2.12 and g = 2.07 Ferroheme–NO EPR Species Present in Fully Reduced SiR-HP Reacted with Nitrite in Various Media[a]

addition to standard buffer	g = 2.12 type signal (R)	g = 2.07 type signal (A)	R + A	total ferro-heme–NO signal
none, $^{14}NO_2^-$	0.68	0.12	0.80	0.78
none, $^{15}NO_2^-$	0.68	0.12	0.80	0.77
0.2 M GdmCl, $^{14}NO_2^-$	0.74	0	0.74	0.74
0.2 M GdmCl, $^{15}NO_2^-$	0.68	0	0.68	0.68
2 M urea, $^{14}NO_2^-$	0.17	0.64	0.81	0.83
2 M urea, $^{15}NO_2^-$	0.18	0.66	0.84	0.85
40% Me_2SO, $^{14}NO_2^-$	0.69	0.03	0.72	0.71
40% Me_2SO, $^{15}NO_2^-$	0.75	0.05	0.80	0.77
60% Me_2SO, $^{14}NO_2^-$	0.31	0.64	0.95	0.91
60% Me_2SO, $^{15}NO_2^-$	0.32	0.60	0.92	0.87

[a] The total amount of ferroheme–NO signal (in spins per SiR-HP) present in each sample of fully reduced SiR-HP plus nitrite was determined by double integration of spectra like those shown in Figure 3. The amplitude of the g = 2.12 feature of each spectrum was compared to that of the 0.2 M GdmCl sample in order to determine the amount of g = 2.07 feature of each spectrum was compared to that of the 2 M urea sample, after subtraction of the indicated amount of g = 2.07 species present.

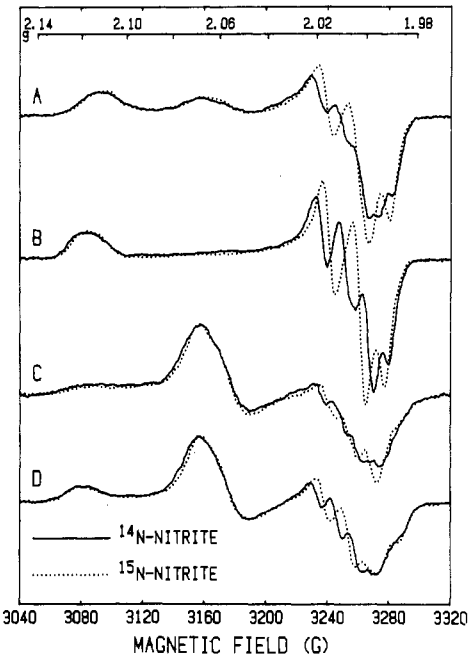

FIGURE 3: EPR spectra of SiR-HP ferroheme–NO complexes in the presence of perturbants. A 10-μL sample of 0.1 M KNO_2 [(—) $^{14}NO_2^-$; (···) $^{15}NO_2^-$] was added anaerobically to EPR tubes containing 62 μM fully reduced SiR-HP, 15 μM Dfl, and 10 mM EDTA in standard buffer containing the indicated additions, in a total volume of 0.2 mL. (A) No additions; (B) 0.2 M guanidinium chloride; (C) 2 M urea; (D) 60% (v/v) dimethyl sulfoxide. EPR spectra were recorded at a temperature of 35 K, 5 mW microwave power, 4 G modulation amplitude, and 9.12 GHz microwave frequency.

nitrogen. The g values of the EPR signal generally resemble those of ferroheme–NO complexes of other hemoproteins and model hemes. Evidence to be presented below shows that the complex nature of the ferroheme–NO EPR spectrum of SiR-HP is due to the presence of two distinct species in the ligated enzyme.

Figure 1 shows that oxidation of the ferroheme–NO complex with ferricyanide yielded a new species with optical maxima at 399 and 581 nm. The optical spectrum of this species is identical with that found upon prolonged incubation of oxidized SiR-HP with NO. The species may therefore be

formally considered as a ferriheme–NO complex, although it may actually be present as ferroheme–NO_2^- or a mixture of the two states. The EPR spectrum of the ferriheme–NO complex, shown in Figure 2C, shows none of the ferroheme–NO signals of the enzyme prior to ferricyanide addition. Instead, the spectrum shows small amounts of an easily saturated novel signal with g = 2.01 and 2.00 (ca. 0.02 spin/heme), as well as minor signals at g = 4.3 (0.08 spin/heme) and g = 6.63 and 5.25 (0.08 spin/per heme). The latter EPR species is due to ferriheme in uncomplexed SiR-HP and undoubtedly represents a small amount of enzyme which has lost its NO (or NO_2^-) ligand.

In the presence of oxygen or excess ferricyanide, the optical and EPR spectra of the ferriheme–NO complex slowly decay to those of the free oxidized enzyme. The rate of this decay can be slowed, but its extent is not changed by raising the concentration of NO_2^- in solution.

The ferriheme–NO complex of SiR-HP can be quantitatively rereduced to the ferroheme–NO species by addition of 1 mM ascorbate, a result which indicates that the reduction potential of this transition is considerably more positive than that of the ferriheme/ferroheme transition in the unligated enzyme.

Accurate quantitation of the number of ferricyanide equivalents actually required to oxidize the ferroheme–NO complex to ferriheme–NO in the experiments of Figures 1 and 2 was complicated by the presence of reducing equivalents reactive with ferricyanide which are generated by the Dfl/EDTA photoreduction system itself, as noted previously by Janick & Siegel (1982, 1983). These reducing equivalents appeared to react with ferricyanide prior to the relatively positive potential ferroheme–NO, leading to a "lag" in the loss of 599-nm absorbance or ferroheme–NO EPR signal as ferricyanide was added in small increments to the ferroheme–NO complex of SiR-HP. By the time 1 equiv of ferricyanide was added to the ferroheme–NO in the experiments of Figures 1 and 2, only a small amount of ferroheme–NO oxidation (20% decrease in g = 2.12 and 2.07 signal intensities) had occurred. However, the formation of the species giving rise to the small g = 4.3 and g = 6.63 and 5.25 EPR signals was essentially complete under these conditions (Figure 2B). Addition of a second equivalent of ferricyanide led to maximal formation of the 581-nm optical species and complete loss of the g = 2.12 and 2.07 EPR signals. These results are consistent with the interpretation tht the transition between the 599- and 581-nm optical species (as well as between the EPR spectral species in the g = 1.9–2.2 region of Figure 2A,C) is in fact a one-electron oxidation of the ferroheme–NO complex of SiR-HP.

Two Types of Ferroheme–NO EPR Signal in SiR-HP. The presence of two distinct features, at g = 2.12 and 2.07, in the EPR spectrum of the SiR-HP ferroheme–NO complex suggested the presence of more than one type of ferroheme–NO species in the enzyme preparation. We found that addition of 0.2 M GdmCl, an agent known to reversibly perturb the EPR spectrum of fully reduced native SiR-HP without altering the exchange-coupled nature of that spectrum [see Janick & Siegel (1983)], caused the EPR spectrum resulting from addition of NO_2^- to photoreduced SiR-HP to show only the g = 2.12, but not the g = 2.07, feature. The spectrum, shown in Figure 3, exhibits g values at 2.117, 2.008, and 1.996, and the resolution of the hyperfine splitting of the g = 2.008 feature is considerably enhanced (A = 15 G for $^{14}NO_2^-$ and 21 G for $^{15}NO_2^-$). Table I shows that the ferroheme–NO signal in the presence of 0.2 M GdmCl accounted for 0.7 spin/SiR-HP, an amount comparable to that in the absence of GdmCl.

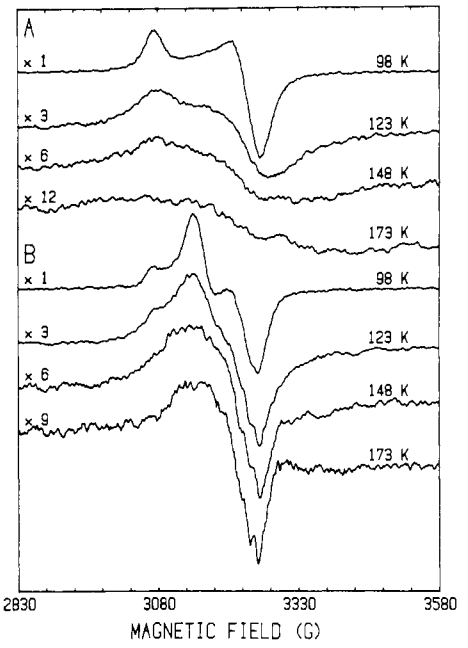

FIGURE 4: EPR spectra of SiR-HP ferroheme–NO complexes as a function of temperature. Spectra of the $^{14}NO_2^-$ samples containing 0.2 M guanidinium chloride (A) or 2 M urea (B) were recorded at the indicated temperatures. Microwave frequency was 9.12 GHz, microwave power was 100 mW, and modulation amplitude was 4 G.

In contrast, Figure 2 shows that the presence of 2 M urea (an agent which causes conversion of the $S = {}^1/_2$ and $S = {}^3/_2$ exchange-coupled EPR signals of fully reduced SiR-HP to one of the g = 1.94 type characteristic of magnetically isolated reduced Fe_4S_4 centers) during photoreduction of SiR-HP led to the appearance of a relatively axial EPR spectrum upon NO_2^- addition with its principal g_1 feature at 2.07, rather than 2.12. The turning points of the primary species formed in the presence of 2 M urea were found at 2.068, 2.054, and 1.997; this species accounted for about 0.65 spin/SiR-HP. As seen in Table I, there was also a small amount (ca. 0.17 spin/SiR-HP) of the GdmCl-type species seen in the urea-treated reduced enzyme–NO complex. The small apparent hyperfine splitting seen on the low-field side of the g = 1.997 feature of the urea spectrum probably corresponds to residual g = 2.12 signal features rather than from actual splitting of the g_3 feature of the g = 2.07 type signal.

Figure 3 and Table I also show that 60% (v/v) dimethyl sulfoxide (which, like 2 M urea, causes the EPR signal of fully reduced unligated SiR-HP to be of the g = 1.94 rather than the exchange coupled $S = {}^1/_2$ or ${}^3/_2$ types) causes the ferroheme–NO EPR spectrum in SiR-HP to be predominately of the near-axial g = 2.07 type. In contrast, 40% (v/v) dimethyl sulfoxide (which does not cause loss of the exchange-coupled $S = {}^1/_2$ type EPR spectrum in fully reduced unligated SiR-HP) leads to an SiR-HP ferroheme–NO spectrum predominately of the rhombic g = 2.12 type.

Examination of the EPR spectra of SiR-HP of SiR-HP ferroheme–NO complexes in native enzyme, in 0.2 M GdmCl, and in 2 M urea as a function of temperature clearly shows that the two types of EPR spectrum observed are not in a temperature-dependent equilibrium with one another. There was little alteration in signal line shape for either the g = 2.12 or 2.07 type species between 35 and 77 K. However, as seen in Figure 4, between 100 and 173 K, both types of signal become severely broadened.

Despite the presence of two distinct types of EPR spectrum for ferroheme–NO in SiR-HP, it should be noted that all of

the conditions used in Figure 3 and Table I yield the 599-nm type of optical spectrum identical with that seen with the native enzyme ferroheme–NO complex.

Ferroheme–NO Complex as a Turnover Intermediate. Nitrite-derived NO binds tightly to two-electron-reduced SiR-HP, since formation of the ferroheme–NO complex of SiR-HP is complete upon addition of stoichiometric quantities of NO_2^- to 5 μM photoreduced SiR-HP. When this SiR-HP ferroheme–NO complex, formed in the absence of excess NO_2^-, was subjected to continued photoreduction in the presence of 1 μM Dfl and 10 mM EDTA, the 599-nm optical spectrum changed to that of partially reduced unligated enzyme (containing about one electron per SiR-HP) over a period of a few minutes, indicating reductive release of the bound NO (presumably as NH_3). No complexes between any reduction state of SiR-HP and NH_3 at NH_4^+ ion concentrations as high as 0.1 M have been detected by either optical or EPR spectroscopy.

When the SiR-HP ferroheme–NO complex was subjected to prolonged photoreduction in the presence of excess NO_2^-, no change in its optical or EPR spectrum was observed (See Figure 2D). Identical optical and EPR spectra (except for the presence of partially reduced flavin species) to those seen with SiR-HP ferroheme–NO were observed when the *E. coli* NADPH–SiR hemoflavoprotein complex was incubated anaerobically with NADPH and excess NO_2^-. In this case, the loss of NADPH could be followed at 340 nm, and the optical and EPR spectra of the ferroheme–NO complex were found to persist after exhaustion of the NADPH. If NADPH was present at more than 3 times the NO_2^- concentration, the spectrum of the ferroheme–NO complex still represented at least 75% of the original enzyme high-spin ferriheme during the course of turnover. As the NO_2^- became exhausted, the EPR and optical spectra reverted to those characteristic of the unligated partially reduced enzyme.

These results indicate that the ferroheme–NO complex is the dominant enzyme species present in the steady state during reduction of NO_2^- to NH_3 catalyzed by SiR-HP. Cammack et al. (1978) and Lancaster et al. (1979) have provided evidence for the participation of the ferroheme–NO species of plant nitrite reductase during catalysis of nitrite reduction (with dithionite as electron donor) by that enzyme.

Kinetics of Formation of SiR-HP Ferroheme–NO Complex. The considerations stated above suggested that the rate-limiting step in catalysis of nitrite reduction by SiR-HP should follow formation of the ferroheme–NO species. It was thus of interest to investigate the kinetics of formation of the complex upon reaction of reduced SiR-HP with NO_2^- to see if the rate of this reaction could be accommodated within the turnover time of the enzyme catalytic cycle.

Figures 5 and 6 show the EPR spectra of samples produced upon reaction of fully photoreduced SiR-HP with 5 mM NO_2^- at 23 °C for various periods of time, followed by rapid freeze quenching of the reaction mixtures at −140 °C. The progress of the reaction clearly involves two sequential steps. The first involves loss of the $S = {}^1/_2$ type EPR signal at $g = 2.53$, 2.29, and 2.07 characteristic of the coupled $S = 1$ or 2 ferroheme–$S = {}^1/_2$ reduced Fe_4S_4 center in the native photoreduced enzyme (Janick & Siegel, 1982) and its replacement by a signal of the $g = 1.94$ type characteristic of a magnetically isolated Fe_4S_4 center. This reaction proceeds with $k_1 = 18.4\ s^{-1}$, and may reflect binding of NO_2^- to the ferroheme to form a low spin ($S = 0$) species. We do not know at present whether or not this reaction involves breaking of the bonds between heme, Fe_4S_4, and the endogenous coupling ligand present in the native

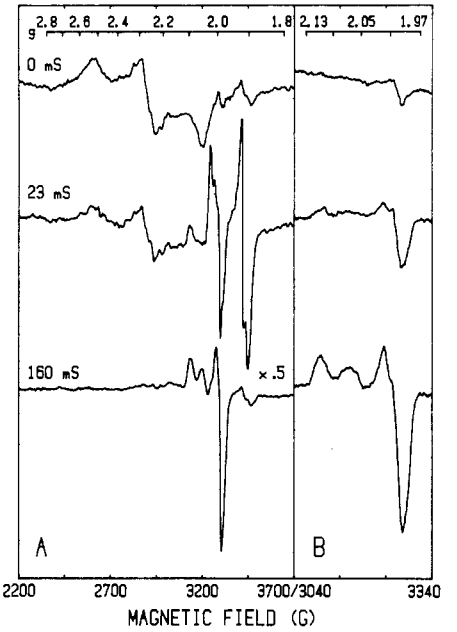

FIGURE 5: EPR spectra observed after rapid mixing of nitrite and fully reduced SiR-HP. An anaerobic solution containing 70 μM SiR-HP, 24 μM Dfl, and 10 mM EDTA in standard buffer was photoreduced in a cuvette designed to permit optical monitoring of the reduction and subsequent anaerobic transfer to a syringe of the Update Instruments Model 1000 rapid mixing system. A second syringe contained an anaerobic solution of either standard buffer (to obtain the zero time point; 23 ms actual reaction time) or 10 mM KNO_2 in standard buffer. The solutions were reacted for the indicated period of time, and the reaction was then rapidly freeze quenched in liquid isopentane at −140 °C. (A) EPR spectra recorded at 20 K temperature and 50 mW microwave power; (B) EPR spectra recorded at 35 K temperature and 5 mW microwave power. Microwave frequency was 9.12 GHz and modulation amplitude was 10 G for all spectra.

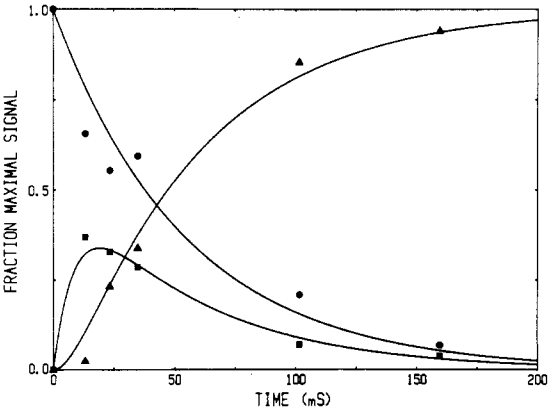

FIGURE 6: Kinetics of the EPR species seen after rapid mixing of nitrite with fully reduced SiR-HP. Data were obtained from the experiment of Figure 5. (●) $g = 2.29$ ($S = {}^1/_2$ type) signal of fully reduced unligated SiR-HP (fraction of original signal present). (■) $g = 1.94$ signal. (▲) $g = 2.01$ signal of ferroheme–NO (fraction of final signal formed). The small amount of $g = 1.94$ signal present in the zero time sample (0.03 spin/SiR-HP) was subtracted from the amount of $g = 1.94$ signal present at each time point. The resultant value (in spins per SiR-HP) is multiplied by a factor of 3 in the figure to facilitate visualization. The small radical signal present in the zero time sample spectrum was likewise subtracted from the $g = 2.01$ feature in all spectra. The lines are theoretical curves for the reaction sequence $g = 2.29 \xrightarrow{k_1} g = 1.94 \xrightarrow{k_2} g = 2.01$ where $k_1 = 18.4\ s^{-1}$ and $k_2 = 115\ s^{-1}$.

enzyme (Christner et al., 1981). The second step involves conversion of the species giving the "$g = 1.94$" type signal to one yielding the $g = 2.12$ and 2.07 signals characteristic of the final ferroheme–NO complex. Note that the two types

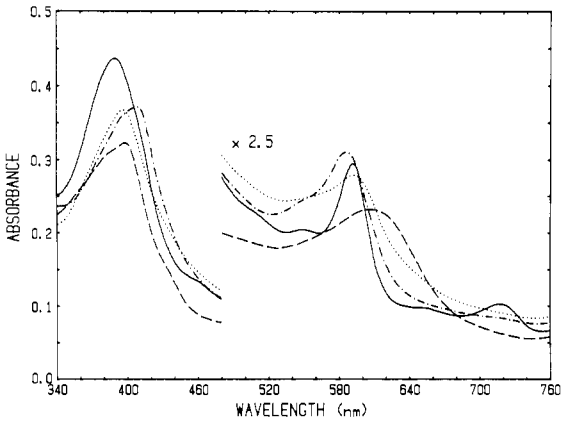

FIGURE 7: Optical spectra of complexes between SiR-HP and sulfite. A solution containing 6.6 μM SiR-HP, 2.6 μM Dfl, and 10 mM EDTA in standard buffer, in a total volume of 0.5 mL, was made anaerobic in the double cuvette apparatus of Janick & Siegel (1982). Spectra were recorded after each of the following operations: (—) oxidized SiR-HP prior to photoreduction; (---) fully reduced SiR-HP (6-min illumination; no optical change was observed during the final 2 min of illumination); (···) 10 μL of 25 mM Na_2SO_3 added to fully reduced SiR-HP; (-·-) 2.0 equiv of $K_3Fe(CN)_6$ added to fully reduced SiR-HP–SO_3^{2-} complex. Optical spectra were corrected for dilution.

of ferroheme–NO signal appear in parallel. This reaction proceeds with k_2 = 115 s^{-1} and probably represents electron transfer from the reduced Fe_4S_4 center to the bound NO_2^-. Because the second step is so much more rapid than the first, only a small amount of the intermediate g = 1.94 species [maximum of 0.13 mol/mol of SiR-HP over and above the 0.03 spin/heme g = 1.94 type signal normally seen in fully reduced native SiR-HP (Janick & Siegel, 1982)] can be detected.

The turnover number for NO_2^- reduction catalyzed by SiR-HP with MV^+ as donor was reported by Siegel et al. (1982) to be equivalent to 16 NO_2^- s^{-1} SiR-HP^{-1} at saturating [NO_2^-]. Since the K_m for NO_2^- is 1.5 mM, one can calculate a turnover number of about 12 NO_2^- s^{-1} SiR-HP^{-1} when 5 mM NO_2^- is used. Thus, the formation of the ferroheme–NO complex can indeed occur rapidly enough (although marginally so at best) to participate in the catalytic cycle of NO_2^- reduction to NH_3.

Complexes of SiR-HP with Sulfite. Siegel et al. (1982) showed that SO_3^{2-} reacts rapidly with SiR-HP only in the presence of a reductant. Figure 7 shows that addition of SO_3^{2-} (in excess) to fully reduced SiR-HP resulted in formation of a species with optical maxima at 396 and 592 nm. EPR examination of this species at a wide range of microwave powers over the temperature range 5–173 K failed to reveal any EPR signals. It is important to note that the spectra showed no significant amounts (<0.02 spin/SiR-HP) of either signals attributable to unligated reduced SiR-HP [see Janick & Siegel (1982)] or signals attributable to oxidized SiR-HP complexed with S^{2-} [see Janick & Siegel (1983)].

The kinetics of the reaction between fully photoreduced SiR-HP and 2 mM SO_3^{2-} were followed by EPR spectroscopy in freeze-quenched samples. The results, shown in Figures 8 and 9, were similar to those seen on reaction of fully reduced SiR-HP with NO_2^-, except that the final state of the enzyme (unlike ferroheme–NO) was EPR silent in the sulfite-reacted SiR-HP. Again, a g = 1.94 type of EPR signal appeared (in a reaction governed by rate constant k_1), reached a maximum of 0.12 spin/SiR-HP, and then disappeared (in a reaction governed by rate constant k_2). The appearance of the g = 1.94 signal coincided with the early stages of the loss of the g = 2.53, 2.29, and 2.07 EPR signals of the native two-electron-

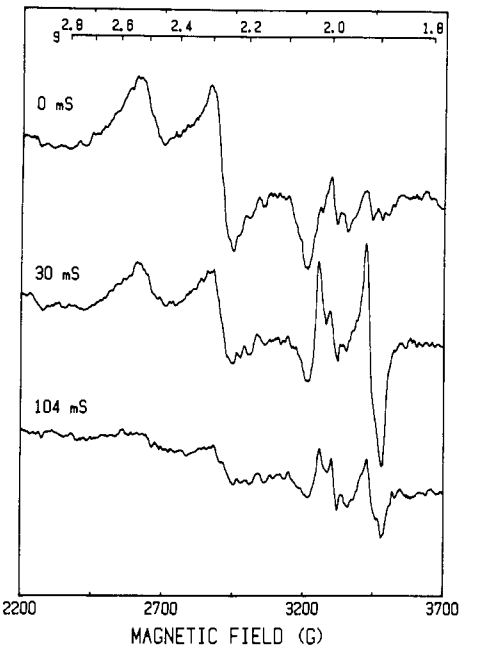

FIGURE 8: EPR spectra observed after rapid mixing of sulfite and fully reduced SiR-HP. The experiment was performed as described in Figure 5, except that 2 mM Na_2SO_3 was substituted for the KNO_2. EPR spectra were recorded at 20 K temperature, 50 mW microwave power, 9.12 GHz microwave frequency, and 10 G modulation amplitude.

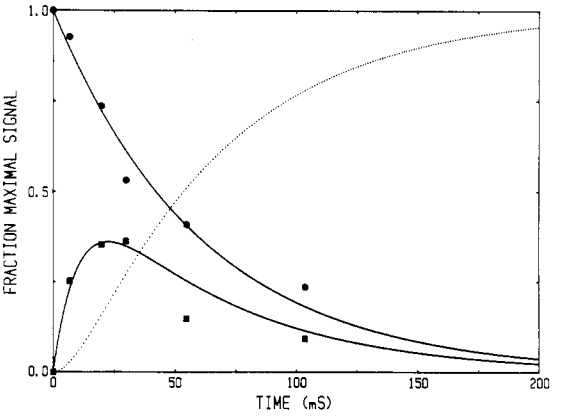

FIGURE 9: Kinetics of the EPR species seen after rapid mixing of sulfite with fully reduced SiR-HP. Data were obtained from the experiment of Figure 8 and were treated as described in Figure 6. (●) g = 2.29 signal (fraction of original signal present). (■) g = 1.94 signal (spins per SiR-HP at a given time minus the 0.03 spin/SiR-HP present in the zero time sample). The lines are theoretical curves for the reaction sequence $g = 2.29 \xrightarrow{k_1} g = 1.94 \xrightarrow{k_2}$ EPR-silent species where k_1 = 16.5 s^{-1} and k_2 = 95 s^{-1}. The dotted curve represents the proportion of the EPR-silent final reduced SiR-HP–SO_3^{2-} complex expected from the scheme given.

reduced enzyme. Since no observable EPR signal results from the product of the reaction, the time course had to be fit by using only the g = 2.29 and g = 1.94 signal intensities. A theoretical fit to the reaction scheme

$$\text{“}g = 2.29\text{” species} \xrightarrow[k_1]{} \text{“}g = 1.94\text{” species} \xrightarrow[k_2]{} \text{EPR-silent species}$$

with k_1 = 16.5 s^{-1} and k_2 = 95 s^{-1}, is shown in Figure 9. The dotted line in Figure 9 represents the amount of EPR-silent species to be expected with the scheme. One may note that the rate constants found for reaction of two-electron-reduced SiR-HP with SO_3^{2-} are similar to those found for its reaction with NO_2^-. It should also be noted that both k_1 and k_2 for the reaction of fully reduced SiR-HP with SO_3^{2-} are greater

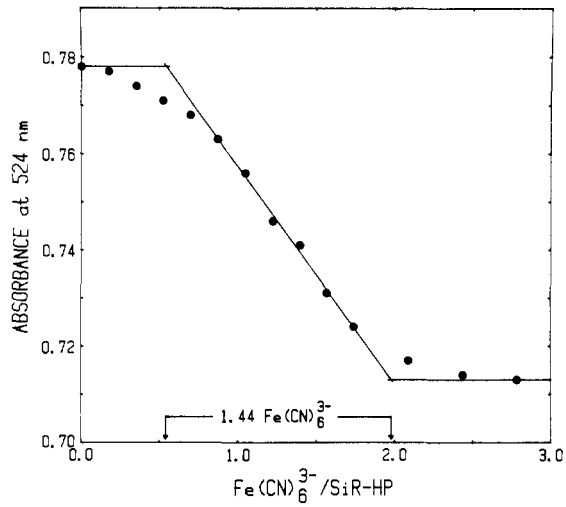

FIGURE 10: Titration of the fully reduced SiR-HP–SO_3^{2-} complex with ferricyanide. A solution containing 55 μM SiR-HP, 11 μM Dfl, 10 mM EDTA, 15 ng/mL bovine liver catalase (Worthington), and 30 ng/mL bovine superoxide dismutate in standard buffer, in a total volume of 0.5 mL, was made anaerobic in the double cuvette apparatus of Janick & Siegel (1982a). Two needles fitted to separate gas-tight syringes, one containing 0.1 M Na_2SO_3 and the other 2.39 mM $K_3Fe(CN)_6$ in standard buffer, were inserted into the apparatus, and the enzyme was then photoreduced until no further change in optical spectrum occurred; 10 μL of the Na_2SO_3 solution was then added, making the solution 2 mM in SO_3^{2-}, and the optical spectrum was recorded. Aliquots of the ferricyanide solution were then added, and the optical spectrum was recorded after each addition. The absorbance at 524 nm (corrected for dilution) is plotted as a function of the amount of ferricyanide added. The linear portion of the plot was fit by a least-squares regression procedure to yield the 1.44 $Fe(CN)_6^{3-}$ per SiR-HP indicated in the figure.

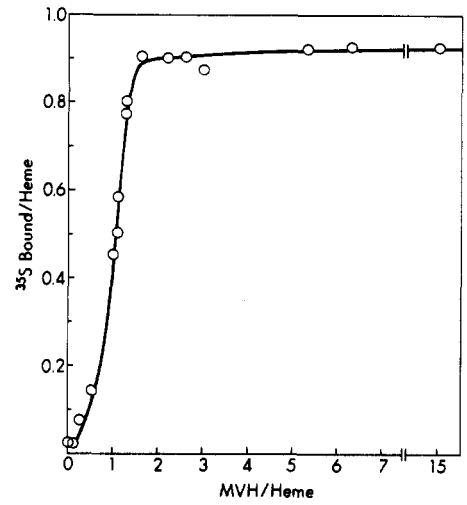

FIGURE 11: Binding of [^{35}S]sulfite to SiR-HP: dependence on MV^+/heme ratio. Solutions, 0.45 mL, containing 8 μM SiR-HP and 0.1 mM $Na_2{}^{35}SO_3$ (specific radioactivity 1.4×10^7 cpm/μmol) in standard buffer were made anaerobic by bubbling with O_2-free Ar. Aliquots of 0.05 mL of MV^+ at concentrations appropriate to yield the ratios of MV^+/heme indicated were then added while bubbling with Ar was maintained. After a 60-s incubation, the solutions were opened to air and subjected to gel filtration on columns of Sephadex G-25, and the protein-associated ^{35}S was determined.

than the maximum turnover number for SO_3^{2-} reduction to S^{2-}, with MV^+ as electron donor, catalyzed by SiR-HP, 7.2 SO_3^{2-} s^{-1} $SiR\text{-}HP^{-1}$, obtained from the data of Siegel et al. (1982).

Figure 7 shows the optical spectrum obtained upon addition of ferricyanide (2 mol/mol of heme) to the complex between fully reduced SiR-HP and SO_3^{2-}. This oxidized species exhibited absorption maxima at 408 and 583 nm and, like the reduced enzyme–SO_3^{2-} complex, yielded no EPR signals [other than those due to small amounts of oxidized unligated enzyme (ca. 0.05 spin ferriheme/SiR-HP)] upon examination at a wide variety of temperatures and microwave powers. The oxidized species was not reduced by ascorbate, indicating that its reduction potential is more negative than that of the oxidized SiR-HP complex with NO. The oxidized SiR-HP–SO_3^{2-} complex was stable upon addition of air or excess $Fe(CN)_6^{3-}$.

Titrations of the fully reduced SiR-HP–SO_3^{2-} complex with $Fe(CN)_6^{3-}$ have yielded data which cannot be interpreted in a simple fashion at present. A typical titration, with the absorbance change at 524 nm plotted as a function of added ferricyanide, is shown in Figure 10. The titration is clearly biphasic, exhibiting a lag phase amounting to some 0.5 $Fe(CN)_6^{2-}$ per SiR-HP and a linear phase of absorbance change extrapolating to 1.44 $Fe(CN)_6^{2-}$ per SiR-HP. Despite the presence of the multiple phases and the fact that more than 1 mol of $Fe(CN)_6^{3-}$ seems to be involved in the oxidation process, the optical spectra observed during the titration yielded no evidence for species other than the fully reduced and fully oxidized SiR-HP–SO_3^{2-} complexes. At least some of the lag may be attributed to the presence of low potential reducing equivalents associated with the Dfl/EDTA photoreducing system itself, as described by Janick & Siegel (1982). However, all titrations have indicated the involvement of significantly more than one ferricyanide per heme in the linear phase of the oxidation process. Thus, one may tentatively conclude that the observed oxidized SiR-HP complex with SO_3^{2-} is at least one and very possibly two electrons more oxidized than the complex formed by reaction of SO_3^{2-} with two-electron-reduced SiR-HP.[2] This species will be characterized in more detail below.

Following addition of stoichiometric amounts of sulfite to 25 μM fully reduced SiR-HP, further Dfl/EDTA photoreduction led to reductive removal of the bound sulfur group (as S^{2-}?) with restoration of the optical and EPR spectra characteristic of fully reduced unligated SiR-HP. Prolonged illumination of the two-electron SiR-HP–SO_3^{2-} complex in the presence of excess SO_3^{2-} resulted in the production of optical species that resembled those described by Janick & Siegel (1983) for partially reduced complexes of SiR-HP with S^{2-}. EPR spectra of such solutions showed the presence of signals with g values at 2.24, 2.21, and 1.96, like those of the oxidized SiR-HP–S^{2-} complex.

Characterization of the Oxidized SiR-HP–SO_3^{2-} Complex. Siegel et al. (1982) found that SiR-HP forms a complex containing 1.0 ^{35}S per heme when incubated with MV^+ and excess $^{35}SO_3^{2-}$. This complex, EPR silent with absorption maxima at 408 and 583 nm, is spectroscopically identical with the more oxidized of the two SiR-HP–SO_3^{2-} species reported above. Taking advantage of the fact that this complex is both stable to air and retains its ^{35}S following gel filtration, we have sought to define the oxidation state and some of the reactivity properties of its bound sulfur moiety.

Sulfite Binding to SiR-HP in the Presence of MV^+. When the concentrations of SiR-HP and $^{35}SO_3^{2-}$ were kept constant (with SO_3^{2-} in excess over MV^+ in all cases), it was found that

[2] We have found that a species with an optical spectrum identical with that seen on $Fe(CN)_6^{3-}$ oxidation of fully reduced SiR-HP–SO_3^{2-} complex can be generated by addition of excess SO_3^{2-} to anaerobic solutions of SiR-HP photoreduced to the one-electron average state of reduction. Complex formation in this case appears to be complete within seconds. We must presume that the one-electron-reduced SiR-HP–SO_3^{2-} complex is thermodynamically unstable under these conditions and is oxidized (by SO_3^{2-}?) to the oxidized SiR-HP–SO_3^{2-} complex.

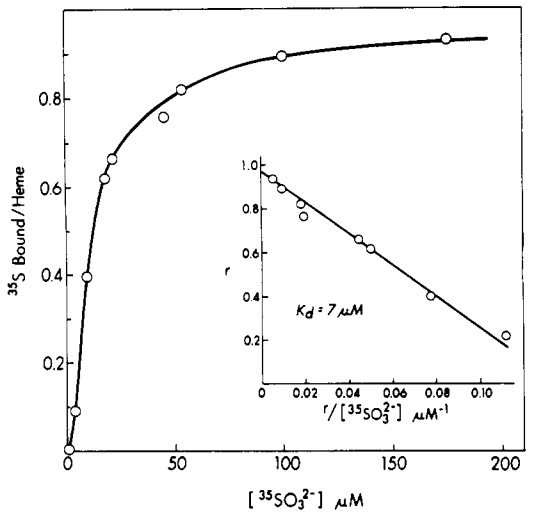

FIGURE 12: Binding of [^{35}S]sulfite to SiR-HP: dependence on [^{35}]sulfite concentration. Solutions, 0.45 mL, containing 8 μM SiR-HP and the indicated concentrations of $Na_2{}^{35}SO_3$ (specific radioactivity 1.1×10^7 cpm/μmol) in standard buffer were made anaerobic by bubbling with O_2-free Ar; 0.05 mL of 0.21 mM MV^+ was injected while Ar bubbling was maintained. After a 60-s incubation period, the solutions were opened to air and subjected to gel filtration on columns of Sephadex G-25, and the protein-associated ^{35}S was measured. (Inset) Scatchard plot of [^{35}S]sulfite binding to MV^+-treated SiR-HP. r = ^{35}S bound per heme. $[^{35}SO_3^{2-}]$ = sulfite concentration corrected for bound ^{35}S and the small amount of added [^{35}S]sulfite reduced to $H_2{}^{35}S$ (radioactivity volatile at pH 7.7).

just over 1 mol of MV^+/mol of heme was required to obtain maximum binding of ^{35}S (Figure 11).

Figure 12 shows that when SiR-HP and MV^+ concentrations were kept constant (the MV^+/SiR-HP ratio was kept small enough so that almost no $^{35}SO_3^{2-}$ was converted to H_2S at the $^{35}SO_3^{2-}$ concentrations used), the amount of ^{35}S bound per heme is a function of the concentration of $^{35}SO_3^{2-}$ present. The inset to Figure 12 shows a Scatchard plot of the binding data, which indicates the presence of one ^{35}S binding site per heme and an apparent dissociation constant for the SiR-HP–$^{35}SO_3^{2-}$ complex of 7 μM.

For the experiments described above and a later experiment (Figure 14), absorption spectra were recorded on all samples for which ^{35}S binding was determined. The fraction of enzyme which exhibited the spectral features of the sulfite complex was determined from the ratio of absorbance at 386 nm (the Soret band maximum wavelength of "free" SiR-HP) to that at 402 nm, an isosbestic wavelength for free and complexed SiR-HP. In all cases there was an excellent correlation between the amount of enzyme present in a spectrophotometrically detectable complex and the amount of ^{35}S bound per heme.

Formation of Complex between Sulfite and Oxidized SiR-HP. Although rapid (reaction complete in a few seconds) binding of ^{35}S derived from $^{35}SO_3^{2-}$ to SiR-HP requires the presence of reductant, radioactivity can become slowly bound to SiR-HP in the absence of MV^+. When SiR-HP was incubated anaerobically at 23 °C with 100 μM $^{35}SO_3^{2-}$, the binding of ^{35}S, determined after aerobic gel filtration of the solution, followed pseudo-first-order kinetics with a $t_{1/2}$ of 5.6 h. A maximum of 1.0 ^{35}S per heme was bound (determined after 48 h of incubation), and the optical spectrum of the complexed enzyme was identical with that obtained with the complex formed rapidly in the presence of MV^+.

In order to determine the kinetics of SO_3^{2-} complexation with oxidized SiR-HP, we incubated aliquots of 3 μM enzyme anaerobically at 23 °C with several concentrations (0.05–2.0 mM) of SO_3^{2-} and recorded absorption spectra as a function of incubation time. All reactions were followed for at least eight half-times to ensure that equilibrium had been obtained. Complex formation followed pseudo-first-order kinetics at each SO_3^{2-} concentration used. No burst or lag phases were detected in any of the time courses. The spectrophotometrically determined $t_{1/2}$ for complex formation at 100 μM SO_3^{2-} was identical with that determined in the previous experiment by using radioactivity measurements at the same concentration of $^{35}SO_3^{2-}$.

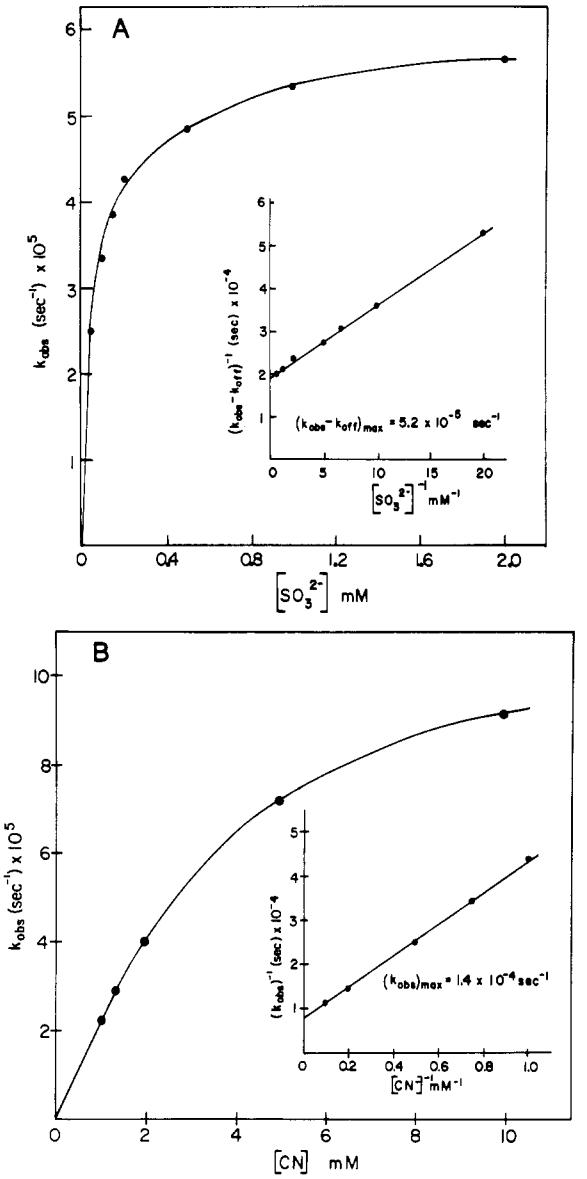

FIGURE 13: Kinetics of spectrophotometrically detectable complex formation between sulfite or cyanide and oxidized SiR-HP as a function of ligand concentration. Solutions of 1.2 mL of 3 μM SiR-HP in standard buffer containing the indicated concentrations of Na_2SO_3 or KCN were incubated anaerobically at 23 °C. Absorption spectra were recorded at various times, and the fraction of total SiR-HP complexed with SO_3^{2-} or CN^- was determined as described under Experimental Procedures. Incubation of each solution was continued until no change in spectrum was observed for at least two half-times. (*A*) Observed first-order rate constants (k_{obsd}) for complex formation between sulfite and oxidized SiR-HP as a function of sulfite concentration. (Inset) A plot of $(k_{obsd}-k_{off})^{-1}$ vs. $[SO_3^{2-}]^{-1}$. For details see the text. (B) k_{obsd} for complex formation between cyanide and oxidized SiR-HP as a function of cyanide concentration. (Inset) Plot of $1/k_{obsd}$ vs. $[CN^-]^{-1}$.

Figure 13A shows a plot of the observed pseudo-first-order rate constants (k_{obsd}) for complex formation between oxidized

SiR-HP and SO_3^{2-} as a function of SO_3^{2-} concentration. It is evident that the kinetics exhibit saturation with respect to SO_3^{2-} as k_{obsd} becomes independent of $[SO_3^{2-}]$ at high SO_3^{2-} concentration.[3]

Dissociation of SiR-HP–Sulfite Complex. Although the complex between SO_3^{2-} and SiR-HP is relatively stable to repeated passage through gel filtration columns, dissociation of sulfite from the complex does occur. Identical results were obtained if the incubation was performed aerobically or anaerobically. Dissociation of 3 μM SiR-HP–$^{35}SO_3^{2-}$ complex, followed both by spectrophotometric measurements and by radioactivity measurements, obeyed apparent first-order kinetics with $t_{1/2}$ = 33 ± 1 h ($k_{off} = 5.8 \times 10^{-6}$ s^{-1}).

By use of the observed k_{off} for the SiR-HP–SO_3^{2-} complex, a double-reciprocal plot of the data for complex formation between SO_3^{2-} and oxidized SiR-HP was constructed as shown in the inset to Figure 13A. A plot of $(k_{obsd} - k_{off})^{-1}$ vs. $[SO_3^{2-}]^{-1}$ yielded an apparent first-order association rate constant for the SO_3^{2-}-independent step in the reaction by extrapolation to zero $[SO_3^{2-}]^{-1}$. The $(k_{obsd} - k_{off})_{max}$ so determined is 5.2×10^{-5} s^{-1}. So that "k_{on}" for the SO_3^{2-}-independent step can be obtained, k_{off} must be added to this value. The true k_{on} is thus 5.8×10^{-5} s^{-1}.

Although the dissociation of the complex formed between SiR-HP and SO_3^{2-} is very slow in standard buffer at 23 °C, the addition of 3.3 M urea under conditions otherwise the same led to complete dissociation of the complex (1–8 μM tested) within 2 min as determined from spectrophotometric and radioactivity measurements. (The dependence of the rate of complex dissociation on urea concentration was not examined in detail. However, when various urea concentrations between 1 and 4 M were tested, 3.0 M urea was found to be the lowest concentration of urea which permitted complete dissociation of the complex within a few minutes.) The enzyme lost little or no ability to catalyze MV^+-dependent reduction of SO_3^{2-} to H_2S following incubation in 3.3 M urea and subsequent dilution into the standard assay system. The solutions of complex treated with 3.3 M urea exhibited spectra identical with those of free SiR-HP in 3.3 M urea (the α band of oxidized SiR-HP in standard buffer is shifted 2–3 nm to lower wavelength in 3.3 M urea).

Oxidation State of Bound S. The rapid and quantitative release of ^{35}S from its complex with SiR-HP in 3.3 M urea provided an opportunity to determine if the sulfur compound released from the complex is indeed at the oxidation level of sulfite. The experiment was performed as follows: 1.0 mL of a solution containing 24 μM SiR-HP–$^{35}SO_3^{2-}$ complex was incubated anaerobically for 5 min in the presence of 3.3 M urea. The solution was then made 120 μM in NADPH and the absorbance at 340 nm recorded. (SiR-HP cannot utilize NADPH as a reductant.) A 1-μL aliquot of 45 μM *E. coli* NADPH–SiR hemoflavoprotein complex was then added and the rapid decrease in A_{340} followed until no further change occurred. The observed ΔA_{340} was corrected for a small absorbance decrease which was consistently observed at this wavelength when the same experiment was performed with free SiR-HP in place of the SiR-HP–SO_3^{2-} complex. In four experiments, the resulting ΔA_{340} corresponded to the oxidation of 66–71 μmol of NADPH, i.e., 2.8 ± 0.1 mol of NADPH/mol of ^{35}S originally bound. Control experiments with standard SO_3^{2-} solutions in the concentration range 20–30 μM used in place of the SiR-HP–SO_3^{2-} complex have shown that a stoichiometry of 2.9 ± 0.1 mol of NADPH/mol of SO_3^{2-} is consistently obtained with *E. coli* NADPH–SiR as catalyst in both standard buffer and buffer containing 3.3 M urea. We may conclude, then, that the sulfur compound released from the SiR-HP–^{35}S complex is in fact at the oxidation level of SO_3^{2-}.

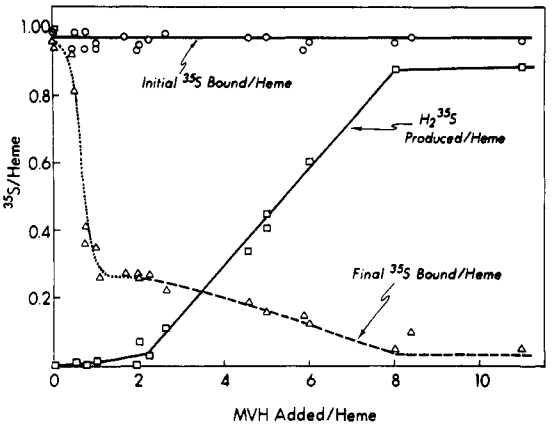

FIGURE 14: Release of ^{35}S from SiR-HP–[^{35}S]sulfite complex upon addition of MV^+. The following procedure was performed at each of the MV^+/heme ratios indicated: A 1.0-mL solution of 8 μM SiR-HP in standard buffer was incubated anaerobically in the presence of 0.1 mM Na_2SO_3 (specific radioactivity 2.68×10^7 cpm/μmol) and 80 μM MV^+ for 1 min at 23 °C. The resulting solution was opened to air and subjected to gel filtration on a column of Sephadex G-25. The eluted protein-bound ^{35}S was determined, and fractions were pooled to give a concentration of 3.8 μM SiR-HP–[^{35}S]sulfite complex. A 1.2-mL solution of complex was bubbled for 10 min with O_2-free Ar to render the solution anaerobic. A 0.02-mL solution of MV^+ at a concentration suitable to yield the desired MV^+/heme ratio was added while bubbling was maintained, and the solution was continuously flushed with O_2-free Ar for 20 min to remove any $H_2{}^{35}S$ formed. A 0.1-mL aliquot of the solution was measured for ^{35}S radioactivity and the amount of $H_2{}^{35}S$ produced per heme calculated by the difference in radioactivity between that of the initial SiR-HP–[^{35}S]sulfite complex and that of the MV^+-treated complex after bubbling. A 1.0-mL aliquot of the bubbled MV^+-treated complex was applied to a column of Sephadex G-25 and the protein-associated ^{35}S determined. (○) Initial ^{35}S bound per heme in original SiR-HP–[^{35}S]sulfite complex. (□) $H_2{}^{35}S$ produced per heme after treatment with MV^+. (△) Final ^{35}S bound per heme after treatment with MV^+. The dashed line represents the theoretical amount of ^{35}S bound per heme expected, assuming a K_D for the SiR-HP–[^{35}S]sulfite complex of 7 μM, if the free and complexed SiR-HP are in equilibrium with a total amount of $^{35}SO_3^{2-}$ equal to the amount of initially added SiR-HP–[^{35}S]sulfite complex minus the amount of $H_2{}^{35}S$ produced at each MV^+/heme ratio used.

Reduction of Bound Sulfite. Rapid release of ^{35}S from its complex with SiR-HP may also be observed upon incubation of the complex with MV^+. However, the form in which the ^{35}S is released and the extent of release of ^{35}S from the complex is dependent upon the MV^+/heme ratio utilized. In this experiment solutions of 3.8 μM SiR-HP–^{35}S in standard buffer (pH 7.7) were incubated anaerobically with various amounts of MV^+ for a 20-min period. During this period each solution was bubbled continuously with O_2-free Ar to remove any volatile radioactivity that had formed during the reaction. At pH 7.7, 10 μM radioactive sulfide can be completely removed

[3] At the highest SO_3^{2-} concentrations utilized in the experiment of Figure 13A, complex formation between SiR-HP and SO_3^{2-} appeared to be complete. At the lowest SO_3^{2-} concentrations utilized, complex formation was clearly not complete even when the incubation period was prolonged until no change in the amount of complex could be detected for at least two reaction half-times. Although data are available only at $[SO_3^{2-}]$ = 50 μM or more, due to the slowness of the reaction between oxidized SiR-HP and SO_3^{2-}, a Scatchard plot of the data available at low $[SO_3^{2-}]$, obtained at apparent equilibrium, was consistent with a reversible binding between oxidized HP and SO_3^{2-} with a dissociation constant of 7 μM. It is of interest that this is the same value for K_D found for the reversible *rapid* binding of SO_3^{2-} to SiR-HP which occurs after incubation in the presence of MV^+.

from solution (as $H_2{}^{35}S$) under these conditions, whereas no loss of radioactive sulfite (which exists as a mixture of $^{35}SO_3^{2-}$ and $H^{35}SO_3^-$ at this pH) could be detected. Aliquots of the resulting solutions were measured for radioactivity remaining and aliquots passed through columns of Sephadex G-25 to remove any unbound but nonvolatile ^{35}S. Both volatile $H_2{}^{35}S$ formed per heme and ^{35}S remaining bound per heme after gel filtration are plotted vs. MV^+ added per heme in Figure 14. It can be seen that upon addition of excess reductant, most of the radioactivity originally bound as $^{35}SO_3^{2-}$ can be released from the complex in the form of volatile $H_2{}^{35}S$. The resulting enzyme exhibits the spectrum of free SiR-HP. In a control experiment 3.8 μM SiR-HP–$^{35}SO_3^{2-}$ and 10 MV^+ per heme were mixed, and the resulting solution was rapidly (without bubbling) analyzed for complex dissociation by both the spectrophotometric and radioactivity techniques. The spectrum of free SiR-HP was seen as soon as the absorption spectrum could be recorded, and less than 0.1 ^{35}S remained bound per heme following gel filtration. Thus, release of ^{35}S from the SiR-HP complex is not a result of the bubbling procedure and is complete in no more than a few seconds. When fewer than 2 mol of MV^+/mol of bound ^{35}S was added to the SiR-HP–$^{35}SO_3^{2-}$ complex in the experiment of Figure 14, a negligible amount of volatile $H_2{}^{35}S$ was released from the complex. We have found this lag phenomenon to be variable in extent; it was significantly decreased (to 0.8 MV^+ per bound ^{35}S) when the concentration of SiR-HP–$^{35}SO_3^{2-}$ complex was raised to 15 μM in an experiment otherwise identical with that of Figure 14. Thus all or part of the observed lag may well be an artifact due to oxidation of small amounts of MV^+ by residual O_2 in the reaction mixtures. This effect would be expected to appear relatively more significant at lower concentrations of SiR-HP–$^{35}SO_3^{2-}$ complex. However, in all experiments, following the lag phase, addition of a further 6 MV^+ per ^{35}S bound resulted in relase of ^{35}S from the complex in 90–95% stoichiometric yields.

Dissociation vs. Reduction of Bound Sulfite. It can be seen in Figure 14 that although reaction of SiR-HP–$^{35}SO_3^{2-}$ complex with small amounts of MV^+ produced little volatile $H_2{}^{35}S$, substantial dissociation of the complex could be detected following addition of no more than 1 MV^+ per heme. In the experiment of Figure 14, treatment of 3.8 μM complex with 1–2 MV^+ resulted in a decrease in the ^{35}S bound per heme from 0.97 to 0.27. If it is assumed in this experiment that the release of ^{35}S at low MV^+/heme ratio follows the reaction $E\text{–}SO_3^{2-} \rightleftharpoons E + SO_3^{2-}$, then a K_D of 7 μM can be calculated from these data. The assumption seems valid since the K_D determined in this manner, based on ^{35}S *dissociation*, is essentially identical with that determined from the Scatchard plot of Figure 12, based on $^{35}SO_3^{2-}$ *binding* data. It should be noted that the apparent equilibrium between bound ^{35}S and *nonvolatile* ^{35}S (presumably SO_3^{2-}) was maintained when more than 2 MV^+ per heme were added to the complex in the experiment of Figure 14. Thus, the dashed line in that figure represents the theoretical curve for the amount of ^{35}S bound per heme to be expected if the SiR-HP is in equilibrium (with a K_D = 7 μM) with a total amount of $^{35}SO_3^{2-}$ equal to the amount of SiR-HP–^{35}S complex initially present minus the amount of volatile radioactivity ($H_2{}^{35}S$) produced at each M v^+ concentration tested. It may be concluded that ^{35}S bound in complex with SiR-HP may be released as either $H_2{}^{35}S$ or $^{35}SO_3^{2-}$ upon reaction of the complex with MV^+.

Since $^{35}SO_3^{2-}$ bound to SiR-HP can be released at low MV^+ or reduced to $H_2{}^{35}S$ at high MV^+, the question is raised as to whether the bound $^{35}SO_3^{2-}$ in the complex as isolated can itself be reduced to $H_2{}^{35}S$, or must it first be released from the enzyme in order to be reduced? The following experiment shows that bound ^{35}S can in fact be reduced independently of exogenous SO_3^{2-} present in solution. In this experiment, excess MV^+ (identical results were obtained with 10, 18, or 36 MV^+ per heme) was added to 3.8 μM SiR-HP–$^{35}SO_3^{2-}$ in the presence of 1 mM nonradioactive SO_3^{2-}. Table II shows that 24 ± 2% of the ^{35}S originally bound was converted to $H_2{}^{35}S$. (About 2% remained associated with the SiR-HP after passage through a column of Sephadex G-25, and the remainder was released from the enzyme as, presumably, $^{35}SO_3^{2-}$.) The resulting SiR-HP solution exhibited the spectrum of the fully formed SO_3^{2-} complex, showing that nonradioactive SO_3^{2-} had replaced the $^{35}SO_3^{2-}$ in the complex with SiR-HP. Thus, the rate of reduction of the bound $^{35}SO_3^{2-}$ must compare favorably with the rate of its release from the enzyme as sulfite in the presence of excess reductant. In a control experiment, 3.8 μM SiR-HP–$^{35}SO_3^{2-}$ was incubated with 2.6 MV^+ per heme in the presence of 1 mM nonradioactive SO_3^{2-} (under these conditions, only a small amount of $H_2{}^{35}S$ was formed). The results shown in Table II demonstrate that bound $^{35}SO_3^{2-}$ is indeed exchangeable with exogenous SO_3^{2-}. At this concentration of MV^+ and in the presence of 1 mM nonradioactive SO_3^{2-}, only 3% of the $^{35}SO_3^{2-}$ originally bound in the complex remained associated with the SiR-HP following gel filtration (while in the absence of nonradioactive SO_3^{2-} about 22% of the original ^{35}S remained bound after gel filtration). The resulting enzyme exhibited the spectrum of the fully formed SiR-HP–SO_3^{2-} complex, indicating that nonradioactive had replaced radioactive SO_3^{2-}. In the absence of reductant (but under otherwise identical experimental conditions) nonradioactive SO_3^{2-} did not rapidly exchange with bound $^{35}SO_3^{2-}$ to any appreciable extent.

Table II: Hemoprotein–[^{35}S]Sulfite Complex: Reduction vs. Dissociation on Treatment with Reduced Methylviologen[a]

MV^+ added per heme	final ^{35}S bound per heme		$H_2{}^{35}S$ produced per heme	
	–sulfite	+1 mM sulfite	–sulfite	+1 mM sulfite
0.0	0.98	0.96	0.00	0.00
2.6	0.22	0.03	0.11	0.08
10.0	0.05	0.02	0.89	0.22
18.0	0.01	0.01	0.93	0.25
36.0	0.00	0.00	0.90	0.22

[a] Hemoprotein–[^{35}S]sulfite complex was prepared as described in Figure 14; 3.8 μM of this complex (specific radioactivity 2.68 × 10^7 cpm/mol) in 1.2 mL of standard buffer or standard buffer containing 1 mM nonradioactive Na_2SO_3 was anaerobically incubated with the indicated amounts of MV^+. $H_2{}^{35}S$ produced per heme and final ^{35}S bound per heme after treatment with MV^+ were determined as described in Figure 14.

Reaction of Oxidized SiR-HP with Cyanide. Siegel et al. (1982) have shown that SiR-HP rapidly forms a tight 1:1 complex with CN^- in the presence of MV^+. This complex could be oxidized in air to give a low-spin ferriheme–CN^- species with a characteristic EPR and optical spectrum. CN^- did not dissociate from either the oxidized or reduced enzyme in standard buffer. Since the optical features of the oxidized SiR-HP–CN^- and SiR-HP-SO_3^{2-} complexes were so similar, and SO_3^{2-} binding and CN^- binding were competitive, it was concluded that both species bound in a similar manner to SiR-HP (probably at the heme).

By incubating various amounts of $^{14}CN^-$ with SiR-HP and MV^+, we found that the amount of complex determined spectrophotometrically (based on the ratio of absorbances at

386 and 404 nm, the latter wavelength being isosbestic for free and CN^--complexed oxidized SiR-HP) correlated well with the amount of complex determined by $^{14}CN^-$ binding following passage through a Sephadex G-25 column.

Cyanide, like SO_3^{2-}, was found to slowly bind to oxidized SiR-HP in the absence of MV^+. The resulting complex contained 1.0 cyanide per heme (determined from an overnight incubation of 4 μM SiR-HP and 100 μM $^{14}CN^-$ in standard buffer at 23 °C following gel filtration) and was spectrophotometrically identical with the complex formed rapidly in the presence of reductant. CN^- binding to oxidized SiR-HP (determined spectrophotometrically) in standard buffer at 23 °C was found to be a pseudo-first-order process at all CN^- concentrations examined (1–10 mM). Complex formation was complete in all cases. Figure 13B shows that the k_{obsd} for CN^- binding to oxidized SiR-HP, like that for SO_3^{2-} binding, becomes independent of ligand concentration at high CN^- concentrations. A plot of $1/k_{obsd}$ vs. $1/[CN^-]$ (inset to Figure 13B) yields the association rate constant (k_{on}) for the CN^--independent first-order process by extrapolation to zero $1/[CN^-]$. The k_{on} so determined (14×10^{-5} s^{-1}) is strikingly similar to that determined for SO_3^{2-} binding to oxidized SiR-HP (6×10^{-5} s^{-1}), particularly when the substantial difference in affinity of SiR-HP for the two ligands is considered.[4]

Discussion

Ferroheme–NO Complexes. Mössbauer and EPR spectroscopy have shown that the heme and Fe_4S_4 centers of SiR-HP are antiferromagnetically exchange coupled in the oxidized and reduced forms of the enzyme (Christner et al., 1981; Janick & Siegel, 1982). This result requires the presence of a ligand chemically bridging the two prosthetic groups in the native enzyme (no exogenously added ligands). The multiplicity of EPR signals found in reduced SiR-HP (Janick & Siegel, 1983) has been interpreted as arising from changes in heme ligation state and/or heme–Fe_4S_4 bonding interactions upon addition of various perturbants. The results found with NO complexes of SiR-HP in this work provide a new probe for examining the ligand arrangements about the heme–Fe_4S_4 center.

Ferroheme–NO complexes of myoglobin (at low temperature) (Morse & Chan, 1980), hemoglobin α chain in the *R* configuration (Hille et al., 1979), cytochrome *c* oxidase (Stevens & Chan, 1981), cytochrome *c* peroxidase, cytochrome *c*, and horseradish peroxidase (Yonetani et al., 1972) all display highly rhombic EPR signals characterized by $g_1 > g_e$, $g_2 = g_e$, and $g_3 < g_e$ (g_2 is interpreted to represent g_z). In these enzymes, the g_2 feature shows not only hyperfine splitting by the NO nitrogen (A = 21 G for ^{14}NO and 30 G for ^{15}NO) but also superhyperfine splitting (A = 6.5 G for ^{14}N) by the nitrogen of the imidazole sixth ligand of these enzymes. Such signals are also typical of imidazole–ferroheme–NO model complexes at $T < 150$ K (Morse & Chan, 1980; Yoshimura et al., 1979). In certain other enzymes, including the hexacoordinate NO complexes of cytochrome P-450 (O'Keefe et al., 1978), chloroperoxidase (Chiang et al., 1975), and lactoperoxidase (Yonetani et al., 1972), only the triplet splitting of g_z is found (but not the superhyperfine splitting). This result has been interpreted as indicating that the NO–ferroheme in these enzymes does not contain a nitrogen atom bound to the Fe^{2+} as part of the sixth ligand (trans to the NO). Rhombic ferroheme–NO EPR spectra have been correlated by X-ray crystallography with an Fe–N–O bond angle of approximately 109° (Hori et al., 1981).

The "g = 2.12" EPR species present in the ferroheme–NO complexes of native SiR-HP (majority species) and enzyme to which 0.2 M GdmCl or 40% dimethyl sulfoxide had been added is clearly rhombic and exhibits triplet splitting by ^{14}NO of its g_2 feature. Conversion of this splitting to a doublet pattern in the ^{15}NO complex demonstrates that the hyperfine interaction is due to the NO nitrogen. No superhyperfine splitting can be detected in the SiR-HP ferroheme–NO EPR spectrum. These results suggest that the NO-ligated heme Fe in SiR-HP is predominately six-coordinate and that the ligand bound trans to the NO does not contain a nitrogen atom (or any other atom with nuclear spin) bound to the heme Fe. (This conclusion must be considered tentative, however, since the presence of unusually rapid electron spin relaxation could prevent detection of superhyperfine splitting if a ligand atom with nuclear spin were present.) Mössbauer spectroscopy of the ferroheme–NO complex of SiR-HP clearly shows magnetic splitting of the oxidized Fe_4S_4 spectrum by the $S = {}^1/_2$ ferroheme–NO at low temperature.[5] Thus the heme and Fe_4S_4 centers of SiR-HP remain exchange coupled, i.e., chemically bridged, when NO is ligated to the heme. If NO is bound to the heme Fe trans to the coupling ligand, then we may tentatively conclude that the coupling ligand does not contain a nitrogen atom bound to the heme Fe. Of course, if NO is not bound to the heme Fe trans to the coupling ligand, then NO itself must be the ligand bridging the heme and Fe_4S_4 centers. [For examples of complexes with metal centers bridged by NO see Connelly (1972).]

The ferroheme–NO complexes of myoglobin, cytochrome *c*, and a number of model heme–imidazole compounds (Yoshimura et al., 1979; Morse & Chan, 1982) have been found to undergo a temperature-dependent equilibrium between two species with markedly different EPR spectra. The temperature study of Figure 7 clearly indicates that the two types of ferroheme–NO EPR signal seen in SiR-HP are not in temperature-dependent equilibrium. At high temperatures, each type of signal simply broadens without obviously changing its basic form. The unusually high degree of broadening seen in the SiR-HP ferroheme–NO spectra at T = 100–175 K suggests that the electron spin relaxation rate is much faster in SiR-HP than in other hemoproteins, a result which may well be due to the presence of an Fe_4S_4 center chemically linked to the ferroheme–NO.

Ferroheme–NO signals of a more axial nature ($g_\perp > g_e$ and $g_\parallel = g_e = g_z$) have been observed with hemoglobin α chains under conditions which favor formation of the T state (Trittelvitz et al., 1975; Hille et al., 1979; Scholler et al., 1979). The hyperfine splitting of the g_z feature goes from a nine- to a three-line species, and infrared (Maxwell & Caughey, 1976) as well as resonance Raman (Strong et al., 1980) spectra have provided evidence which suggests either extreme weakening of the bond between a sixth ligand and the heme Fe or the complete absence of such a ligand in the ferroheme–NO

[4] Oxidized SiR-HP is capable of binding CN^- even in the presence of 3.3 M urea. Although only limited kinetic data are available, CN^- binding, at 2 mM CN^-, in the presence of urea at 23 °C is a much faster process ($t_{1/2}$ = 35 min) than binding with the same concentration of CN^- in the absence of urea ($t_{1/2}$ = 290 min). Although no dissociation of the SiR-HP–CN^- complex could be detected in standard buffer, Siegel et al. (1982) have reported that such dissociation does occur in the presence of 3.3 M urea. Dissociation of 4.6 μM SiR-HP–CN^- complex proceeded as a first-order reaction with a $t_{1/2}$ of 62 min and was accompanied by appearance of MV^+–SO_3^{2-} reductase activity in parallel with CN^- release.

[5] J. A. Christner, E. Munck, P. A. Janick, and L. M. Siegel, unpublished results.

complex. Axial type ferroheme–NO EPR spectra have also been produced by adding denaturing concentrations of NaDodSO$_4$ to hemoglobin (Kon, 1968) or deoxycholate to cytochrome P-450 (O'Keefe et al., 1978). Again, weakening of the coordination of the heme Fe to a sixth ligand has been suggested. A five-coordinate NO–Fe^{2+}–TPP complex has been synthesized and shown to possess an Fe–N–O bond angle of 149° by X-ray crystallography (Scheidt & Frisse, 1975). The EPR spectrum of this complex is of an incompletely resolved type with g_1 and $g_2 > g_e$ and g_3 (interpreted to be g_z) with a three-line hyperfine pattern (Kon, 1975; Wayland & Olson, 1974).

The majority $g = 2.07$ ferroheme–NO EPR signal seen with SiR-HP in the presence of 2 M urea or 60% dimethyl sulfoxide is clearly of the near-axial type, with its high field g feature close to g_e. (Since a small amount of the rhombic $g = 2.12$ type of signal remains, the true position of the high field g value may be even higher than that given.) The comparison of this spectrum with those in the literature suggests that the Fe–N–O bond angle in this form of SiR-HP is probably less bent than that in the majority species of native SiR-HP-NO. There may also be a weaker bond between the heme–Fe and a ligand trans to the NO in SiR-HP–NO in 2 M urea or 60% dimethyl sulfoxide.

Urea and dimethyl sulfoxide were originally selected because they have been shown to promote ligand rearrangement about the heme–Fe$_4$S$_4$ center in SiR-HP, converting the EPR spectrum of fully reduced SiR-HP to one of the $g = 1.94$ type (Janick & Siegel, 1983). Because the ferroheme seems to be largely low spin in the presence of these agents (probably due to addition of an endogenous protein ligand), rendering the heme $S = 0$, one could not tell by EPR spectroscopy whether or not the heme and Fe$_4$S$_4$ centers remained coupled in reduced SiR-HP treated with 2 M urea or 60% dimethyl sulfoxide. Mössbauer spectroscopy of the ferroheme–NO complex of SiR-HP in 2 M urea clearly shows that the heme and Fe$_4$S$_4$ centers remain exchange coupled in the presence of this agent.[5] If the axial EPR spectrum for ferroheme–NO in SiR-HP does indeed represent a five-coordinated heme–Fe, then it would follow that NO must represent the heme–Fe$_4$S$_4$ bridging ligand in the SiR–NO complex in 2 M urea.

Interpretation of the nature of the rhombic vs. axial EPR spectra for the ferroheme–NO complexes of SiR-HP is of particular importance when one examines the ferroheme–NO EPR spectra reported in the literature for plant nitrite reductases (Cammack et al., 1978; Lancaster et al., 1979; Fry et al., 1980). The NiR spectra are clearly of the axial type and are very similar to the $g = 2.07$ species seen in SiR-HP in 2 M urea. The spectra of Fry et al. (1980) show clear evidence for an isotropic hyperfine splitting of the g_z feature in NiR–NO, which is obscured in other preparations by the presence of small amounts of a rhombic species of the SiR-HP type. These results suggest a significant difference in the detailed arrangement of ligands about the heme–Fe in SiR-HP vs. plant NiR.

Kinetic Studies Involving SiR-HP–Substrate Complexes. The turnover studies reported in this paper clearly indicate that the ferroheme–NO complex of SiR-HP is the major species of the enzyme appearing during catalysis of nitrite reduction to NH_3. There is no strong evidence to support an obligatory role for either of the enzyme–SO_3^{2-} complexes reported in this work in catalysis, although it has been demonstrated that the bound substrate can be reductively removed from the oxidized and possibly the two-electron-reduced SiR-HP–SO_3^{2-} complexes.

The rate of formation of the stable complexes between two-electron enzyme and SO_3^{2-} or NO_2^- is marginally fast enough to permit such complexes to be catalytic intermediates. Binding of either substrate to the fully reduced enzyme elicits a change in the EPR spectrum of the coupled-reduced Fe$_4$S$_4$–ferroheme active center. The reduced Fe$_4$S$_4$ becomes magnetically isolated, yielding a $g = 1.94$ type of EPR signal in place of the exchange-coupled set of signals found in unligated reduced SiR-HP. Such a result may reflect either a change in ferroheme spin state from $S = 1$ or 2 to $S = 0$ upon ligation of the heme with substrate or a loss in coupling between the heme and Fe$_4$S$_4$ centers as substrate binds (perhaps displacing the normal bond between coupling ligand and heme present in the native enzyme). The two possibilities are of course not mutually exclusive. The rather slow rate of the initial enzyme–substrate interaction leading to formation of the $g = 1.94$ EPR signal is in keeping with the possibility that substrate binding to the heme does in fact require some significant rearrangement of bonds about the coupled heme–Fe$_4$S$_4$ center. It is also interesting in this regard that the rates of reaction of SO_3^{2-} and NO_2^- with reduced SiR-HP are virtually identical.

Mössbauer spectroscopy[5] of the SiR-HP ferroheme–NO complex (as well as of the oxidized SiR-HP–SO_3^{2-} complex) has clearly shown that exchange coupling between the heme and Fe$_4$S$_4$ centers is maintained in these complexes. Thus, either the original coupling between the centers is maintained throughout the binding and electron transfer reactions or a new coupling ligand, perhaps derived from the substrate itself, has replaced the original bridging group.

It is also of interest that the kinetics of reaction of oxidized SiR-HP with two different ligands, SO_3^{2-} and CN^-, also suggests the presence of a common rate-limiting step (although the rate of this step is some 4–5 orders of magnitude slower than that with the two-electron-reduced enzyme). If this step is not due to a trivial cause, e.g., reaction of enzyme with small amounts of an endogenous reductant to permit substrate binding, it may again reflect a requirement for internal ligand rearrangement (presumably very slow in oxidized enzyme) before external ligands can bind.

Nature of the EPR-Silent SiR-HP–Sulfite Complexes. Although plausible assignments can be made for the reduced and oxidized complexes formed between SiR-HP and NO_2^-, i.e., ferro- and ferriheme–NO, respectively, this has proven difficult for the analogous complexes between SiR-HP and SO_3^{2-}. The product of the reaction between two-electron-reduced SiR-HP and SO_3^{2-} is quite stable under anaerobic conditions, although it can be readily reduced when additional reducing equivalents become available. Since formation of this species involves loss of the reduced Fe$_4$S$_4$ center EPR signal(s), it may be presumed that electron transfer has occurred from the reduced Fe$_4$S$_4$ center to the ferroheme–SO_3^{2-} complex. The product of this reaction might plausibly be either ferroheme–SO_2^{-}·, a potentially highly reducing species, or ferriheme–SO_2^{2-}, a somewhat less reactive species. In either case, an EPR signal would be expected; the absence of such a signal remains to be explained.

Equally puzzling is the absence of an EPR signal (at ≥ 5 K) in the oxidized SiR-HP–SO_3^{2-} complex, a species whose optical spectrum suggests it contains low-spin ferriheme, and which appears to contain S at the oxidation level of SO_3^{2-}. Preliminary Mössbauer spectra of this complex[5] show that the heme is indeed magnetic, but with parameters suggestive of high-spin rather than low-spin ferriheme. The Fe$_4$S$_4$ center is in the 2+ (oxidized) state in this complex, and appears to

still be magnetically exchange coupled to the ferriheme. Although the number of oxidizing equivalents required to convert the two-electron-reduced SiR-HP-SO_3^{2-} complex to the oxidized complex has not yet been totally defined, it is clear that this number is greater than 1 and is more likely to be 2. The ability of the oxidized SiR-HP-SO_3^{2-} complex to form in the absence of reductants (albeit slowly) suggests (though it by no means proves) that this complex is fully oxidized. The one-electron-reduced SiR-HP-SO_3^{2-} complex appears to be intrinsically unstable, being readily oxidized in the presence of excess SO_3^{2-} to the fully oxidized SiR-HP-SO_3^{2-} species. The fate of the electron in this process has not been established.

Registry No. Sulfite, 14265-45-3; nitrite, 14797-65-0; cyanide, 57-12-5; NADPH–sulfite reductase, 9029-35-0.

References

Aasa, R., & Vangaard, T. (1975) *J. Magn. Reson. 19*, 308–315.

Barber, M. J., & Salerno, J. C. (1980) in *Molybdenum and Molybdenum-Containing Enzymes* (Coughlin, M. P., Ed.) pp 543–568, Pergamon Press, Oxford.

Bray, R. C. (1961) *Biochem. J. 81*, 187–193.

Cammack, R., Hucklesby, D. P., & Hewitt, E. J. (1978) *Biochem. J. 171*, 519–526.

Chiang, R., Makino, R., Spomer, W. E., & Hagar, L. P. (1975) *Biochemistry 14*, 4166–4171.

Christner, J. A., Munck, E., Janick, P. A., & Siegel, L. M. (1981) *J. Biol. Chem. 256*, 2098–2101.

Connelly, N. G. (1972) *Inorg. Chim. Acta, Rev. 6*, 47–89.

Fry, I. V., Cammack, R., Hucklesby, D. P., & Hewitt, E. J. (1980) *FEBS Lett. 111*, 377–380.

Hille, R., Olson, J. S., & Palmer, G. (1979) *J. Biol. Chem. 254*, 12110–12120.

Hori, H., Ikeda-Saito, M., & Yonetani, T. (1981) *J. Biol. Chem. 256*, 7849–7855.

Janick, P. A., & Siegel, L. M. (1982) *Biochemistry 21*, 3538–3547.

Janick, P. A., & Siegel, L. M. (1983) *Biochemistry* (in press).

Kon, H. (1968) *J. Biol. Chem. 243*, 4350–4357.

Kon, H. (1975) *Biochim. Biophys. Acta 379*, 103–113.

Krueger, R. J., & Siegel, L. M. (1982) *Biochemistry 21*, 2892–2904.

Lancaster, J. R., Vega, J. M., Kamin, H., Orme-Johnson, N. R., Orme-Johnson, W. H., Krueger, R. J., & Siegel, L. M. (1979) *J. Biol. Chem. 254*, 1268–1272.

Massey, V., & Hemmerich, P. (1978) *Biochemistry 17*, 9–17.

Maxwell, J. C., & Caughey, W. S. (1976) *Biochemistry 15*, 388–396.

Morse, R. H., & Chan, S. I. (1980) *J. Biol. Chem. 255*, 7876–7882.

O'Keefe, D. H., Ebel, R. E., & Peterson, J. A. (1978) *J. Biol. Chem. 253*, 3509–3516.

Scheidt, W. R., & Frisse, M. E. (1975) *J. Am. Chem. Soc. 97*, 17–21.

Scholler, D. M., Wang, M. R., & Hoffman, B. M. (1979) *J. Biol. Chem. 254*, 4072–4078.

Siegel, L. M., & Davis, P. S. (1974) *J. Biol. Chem. 249*, 1587–1598.

Siegel, L. M., Murphy, M. J., & Kamin, H. (1973) *J. Biol. Chem. 248*, 251–264.

Siegel, L. M., Murphy, M. J., & Kamin, H. (1978) *Methods Enzymol. 52*, 436–447.

Siegel, L. M., Rueger, D. C., Barber, M. J., Krueger, R. J., Orme-Johnson, N. R., & Orme-Johnson, W. H. (1982) *J. Biol. Chem. 257*, 6343–6350.

Stevens, T. H., & Chan, S. I. (1981) *J. Biol. Chem. 256*, 1069–1071.

Stolzenberg, A. M., Strauss, S. H., & Holm, R. H. (1981) *J. Am. Chem. Soc. 103*, 4763–4778.

Strong, J. D., Burke, J. M., Daly, P., Wright, P., & Spiro, T. G. (1980) *J. Am. Chem. Soc. 102*, 5815–5819.

Thorneley, R. N. F. (1974) *Biochim. Biophys. Acta 333*, 487–496.

Trittelvitz, E., Gersonde, K., & Winterhalter, K. H. (1975) *Eur. J. Biochem. 51*, 33–42.

Wayland, B. B., & Olson, L. W. (1974) *J. Am. Chem. Soc. 96*, 6037–6041.

Yonetani, T., Yamamoto, H., Erman, J. E., Leigh, J. S., Jr., & Reed, R. H. (1972) *J. Biol. Chem. 247*, 2447–2455.

Yoshimura, T., Ozaki, T., Shintani, Y., & Watanabe, H. (1979) *Arch. Biochem. Biophys. 193*, 301–313.

Zamenhof, S. (1957) *Methods Enzymol. 3*, 702.